MDPI

Article

Determination of the required Power Response of Inverters to provide fast Frequency Support in Power Systems with low Synchronous Inertia

Alejandro Rubio [1,*], Holger Behrends [1], Stefan Geißendörfer [1], Karsten von Maydell [1] and Carsten Agert [1]

[1] DLR Institute of Networked Energy Systems, Carl-von-Ossietzky-Str. 15, 26129 Oldenburg, Germany; holger.behrends@dlr.de (H.B.); stefan.geissendoerfer@dlr.de (S.G.); karsten.maydell@dlr.de (K.M.); carsten.agert@dlr.de (C.A.)

* Correspondence: alejandro.rubio@dlr.de; Tel.: +49-441-99906-481

Version December 17, 2019 submitted to Energies

Abstract: Decommissioning of conventional power plants and the installation of inverter-based renewable energy technologies decrease the overall power system inertia, increasing the rate of change of frequency of the system (RoCoF). These expected high values of RoCoF shorten the time response needed before load shedding or generation curtailment takes place. In a future scenario where renewables are predominant in power systems, the ability of synchronous machines to meet such conditions is uncertain in terms of capacity and time response. The implementation of fast power reserve and synthetic inertia from inverter-based sources was assessed through the simulation of two scenarios with different grid sizes and primary reserve response. As main results it was obtained that full activation time for fast power reserve with penetration above 80% of inverter-based generation would need to be 100 ms or less for imbalances up to 40% regardless of the synchronous response and grid size; meaning that current frequency measurement techniques and the time for fast power reserve deployment would not ensure system stability under high unbalanced conditions. At less unbalanced conditions, the grid in the European scale was found to become critical with imbalances starting at 3% and non-synchronous share of 60%.

Keywords: fast power reserve, frequency nadir, critical time, low inertia grids

1. Introduction

As part of the international efforts set to counteract global warming, the deployment of renewable energies in the electric sector has been considered an energetic priority as a measure to reduce CO_2 emissions. This objective is also reflected in the regulatory energy policies and plans of some countries. For instance, in Germany, the transformation of the electricity sector contemplates achieving a share of electricity generation of 80% from renewable energy by 2050. As part of such transformation, the expansion of renewables and the decommissioning of conventional power plants is regulated by the "Erneuerbare Energien Gesetz" [1].

Decommissioning conventional power plants and its replacement with inverter-based renewable power plants has as an effect the reduction of system inertia; and consequently the increment of RoCoF values. The relevance of system inertia is to avoid rapid changes in frequency as load-generation imbalances take place; in this way, enough time is given for the activation of the primary power reserve to recover the balanced stable conditions. Currently in Germany, the commitment of renewable energy plants has dispatch priority in the power market due to its zero marginal cost for power

generation. This affects market auctions and also technical implications [2]. Balancing of the residual load is provided by conventional units, so curtailment of renewable energy resources is the least preferred option for power balancing [3]. As an immediate result of an imbalance between generation and load, the system frequency starts deviating from its rated value. In continental Europe, the range between 49.8 Hz and 50.2 should be maintained by reserves after a power imbalance. This frequency range corresponds to the ordinary operation range. The primary reserve of the interconnected system can withstand a power imbalance of 3 GW when the system has a total load of 150 GW [4]. At the European level, the reference incident case scenario of power loss of 3 GW has been found adequate even with high penetration of renewables [3,4]. Nevertheless, there will be still many hours with positive residual load and due to the decommissioning of conventional power plants; their diminished capacity to provide balancing power services at such low inertia levels will have to be compensated by balancing services coming from renewables/storage. Additionally to the uncertainty of conventional generation availability in the German power system, it is also not clear whether instantaneous reserve services from abroad would be available and if transmission capacities will be enough for such [3].

Some ancillary services have been included in the inverter's capabilities; inverter-based generation from PV has been employed to contribute to voltage regulation by providing reactive power to the grid. Similarly, other approaches have been implemented for over frequency cases, by curtailment implementation and ramping limitation of inverters when the system frequency approaches an upper limit defined by local codes [5,6]. In the same sense, new techniques have been developed to enable inverter-based generation, such as PV and wind, to also participate in frequency support for under-frequency cases. The most common techniques try to emulate the droop power-frequency characteristic of the synchronous machine by leaving some power headroom during normal operation. Then when a system frequency sag occurs, the inverter can push part of the total available headroom power to counteract the frequency drop [7]. Hence, renewable sources are not any longer operating at their maximum power point, these methods also have some economic constraints. Another approach to limit the frequency drop during the seconds after an event leading to a frequency decay is to mimic the inertial response of synchronous machines. Since PV systems do not count with rotating masses, this approach is only achievable with wind turbines and called synthetic or hidden inertia. Due to the decoupling of wind turbines from the grid dynamics, modified control strategies in the power electronics allows the controller to extract part of the stored kinetic energy in the rotating masses of the wind turbine by adjusting the electromagnetic torque in the generator [7].

Although the integration of more inverter-based generation causes higher values of RoCoF, they also present the solution with the implementation of fast power reserve for frequency support. Whereas synchronous power reserve deployment is in the order of few seconds (5-30s), power electronics implementation offer full power deployment in the order of milliseconds [8]. In this investigation, the conditions which should be fulfilled by inverters in highly penetrated grids by non-synchronous generation, to provide an inverter-based fast power reserve (IBFPR) are investigated. Then the required triggering time and power response to avoid under-frequency load shedding (UFLS) are estimated. The over-frequency phenomenon is treated with the same approach as the under-frequency case. The effectiveness of synthetic inertia is evaluated under some assumed future scenario conditions. Two grid cases are utilized to assess the influence of the grid size, synchronous response and common simplifications made in power system analysis. The IEEE 9 bus benchmark grid model and an electric power system in the European scale are considered for such purpose; a methodology to determine the requirements of the fleet of inverters to offer frequency support is developed.

2. Methodology

2.1. Frequency limits and Inertia Constants

When the global security of the system is endangered and under/above frequency is experienced, the load shedding is activated; the system is said to be in the emergency state. If the frequency exceeds the range between 47.5 and 51.5 Hz, a system blackout can hardly be avoided [4]. Consequently, the system will reach the so-called blackout state and will have to be restored. Before the blackout, the system tries to recover the balance by rejecting partial load starting at 49 Hz as frequency decreases. On the other hand, curtailment thresholds between 50.2 and 50.5 Hz have been studied by ENTSOE for over-frequency scenarios [4]. In this research, a deviation of ± 1 Hz is used as a threshold before load shedding and curtailment starts. Hence, to keep frequency within such threshold; the investigated critical time and power response, corresponding to the maximum allowed time for fast power reserve activation. In the case of under-frequency power is injected in the system whereas, in the over-frequency case, power is extracted from the grid.

Two terms commonly found in the literature of power system stability will be used along this section:

- **Inertia constant (H)**: It has units of seconds (s) and it is the ratio of the stored kinetic energy in the rotating masses of the machine (E_k in MWs) and its nominal capacity (S_{nom} in MVA).

- **Acceleration time constant (T_a)**: It also has the units of seconds (s) but this is the ratio of double the kinetic energy (MWs) and the generator nominal power output (P_{nom} in MW).
  Acceleration time constant is a measure of the robustness against disturbances of the system. It could be interpreted as the required time to remove the kinetic energy from the rotating masses of the generators connected in a grid at the rate of the supplied power load. Hence, the higher the time constant, the higher the kinetic energy available. As the share of synchronous generations decreases, this constant decreases proportionally.

With f as frequency, f_0 as nominal frequency and ΔP as power imbalance, the swing equation can be expressed as follows [9]:

$$\frac{df}{dt} = \frac{\Delta P * f_0}{2 * H * S_{nom}} = \frac{\Delta P * f_0}{T_a * P_{nom}} = \frac{\Delta P * f_0}{2 * E_k} \tag{1}$$

In this paper, the inertia constant H is used for the description of inertia in wind turbines and single synchronous machine representation whereas the system acceleration constant T_a is used to express the whole system inertia related to the load in terms of real power.

2.2. Frequency Support from Inverter based Generation

In this section, the methodology and considerations for the implementation of inverter-based generation for frequency support are explained.

2.2.1. Synthetic Inertia

Synthetic inertia is one of the techniques that manufactures and researchers are considering to tackle the low inertia problem in power systems [10,11]. Frequency support through synthetic inertia was considered with the following assumptions [7,12]:

1. Power output from synthetic inertia is limited to 10% of the wind turbine nominal power.
2. Due to mechanical and thermal stresses, the additional power can be delivered only for a maximum time of 10 s.
3. It is assumed that all wind turbines operate at its nominal power output. The value of 1.5 MW was selected for such purpose.

4. The maximum allowable amount of kinetic energy to be extracted from the turbines was limit to half of the kinetic energy while the turbine operates at nominal speed [13].

A control system is needed so the stored energy in the rotating blades can be extracted from the wind turbine. Using the expression of power as the derivative of the stored energy in the blades Equation (2) is obtained. The additional extracted power from the wind turbine through the implementation of Equation (2) accounts for the synthetic inertia contribution [13].

$$P_{pu}(t) = 2 * H_{wt} * \omega_{pu}(t) * \frac{d\omega_{pu}(t)}{dt} \tag{2}$$

Where H_{wt} is the turbine inertia constant and ω_{pu} the rotational speed in per unit.

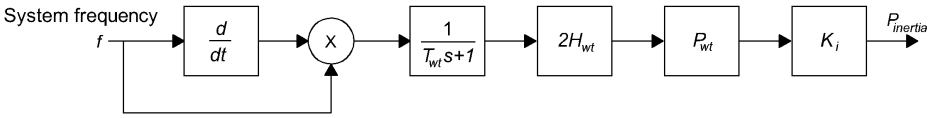

Figure 1. Representation of Equation (2) in Simulink. In the figure it can be seen the insertion of a filter at the output of the multiplication block [11,12]. A constant block K_i adjusts the initial response in the model. Since Equation (2) is given in pu, the output is multiplied by a constant P_{wt} representing the rated power of the turbine.

Typical values of inertia constant for wind turbines are not openly available from the manufacturers to the public. The approximate value was calculated with the utilization of an equation which relates nominal power and inertia constant for wind turbines [14].

$$H_{wt} \approx 1.87 * P_{nwt}^{0.0597} \tag{3}$$

For a wind turbine with a nominal power output of 1.5 MW, the value of H corresponds to 4.37 s [15]. Rated rotational speed of 18 rev/min was considered [15]. To avoid the wind turbine to stall, a reduction of 5 rev/min is allowed by the implementation of the control system. This change of rotational speed equals a reduction of 3 MWs on kinetic energy out of a total of 6 MWs.

Table 1. : Constants for the implementation of synthetic inertia in Simulink, n_{wt} represents the number of wind turbines with synthetic inertia control

T_{wt}	H_{wt} (s)	P_{wt} (MW)	K_i
1	4.37	1.5*n_{wt}	10

2.2.2. Inverter based fast Power Reserve

When a power system is subjected to a negative power imbalance and it is assumed that no load is rejected at UFLS frequency, this continues dropping below 49 Hz. The time at which the system frequency equals the UFLS value is then called critical time. This is the maximum available time for the inverter based reserve to deploy the required power to the system.

In the critical condition that would lead to load shedding, it is expected from the IBFPR to at least counteract the RoCoF at the critical time, as illustrated in Figure 2b. Recalling Equation (1); it is necessary that the machine accelerating power (power imbalance) become zero at the critical time.

$$P_a(t_{cr}) = P_{mech} - P_{elec} + P_{IBFPR} = 0 \tag{4}$$

Where P_a is accelerating power, P_{mech} is mechanical power, P_{elec} is electrical power load, t_{cr} is the critical time and P_{IBFPR} is inverter based fast power reserve.

From the assumption of a linear mechanical power deployment of the synchronous machines governors, the rate of change in mechanical power, after a power imbalance ΔP, is given by $\Delta P / t_{nadir}$,

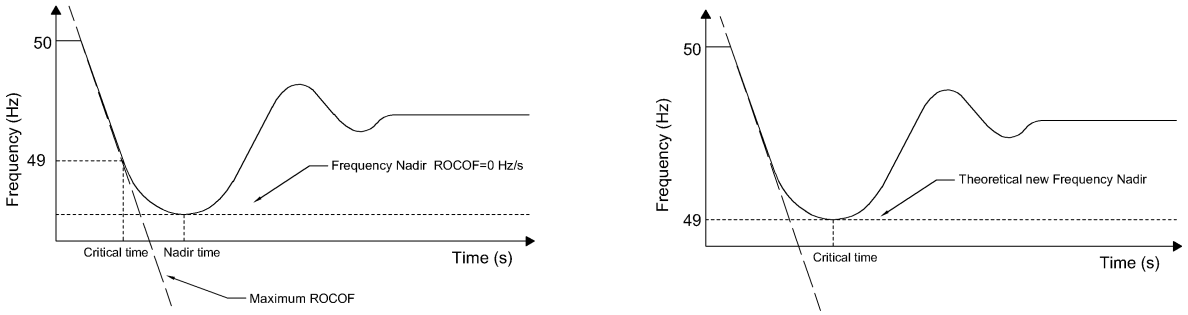

(a) Without IBFPR **(b)** With IBFPR

Figure 2. In (**a**) the frequency response goes below the 49 Hz leading to UFLS at the critical time, whereas in (**b**) the IBFPR is applied to avoid ULFS. In this case, the power imbalance is compensated at the critical time by the inverters.

where t_{nadir} represents the time at which the frequency nadir occurs. Given the power balance at the critical time, t_{cr}; the IBFPR response must be equal to $P_{elec} - P_{mech}$, being P_{elec} equal to ΔP.

Substituting P_{mech} by $\Delta P * t_{cr}/t_{nadir}$ and P_{elec} by ΔP in Equation (4), the following expression is obtained for the P_{IBFPR} at time t_{cr}:

$$P_{IBFPR}(t_{cr}) = \Delta P * (1 - t_{cr}/t_{nadir}) \tag{5}$$

It is assumed that P_{IBFPR} remains with a constant power output after t_{cr} long enough to stabilize the system frequency. The result of the previous equation represents the slope of the power output since the inception of the incident until the critical time, which with the implementation of IBFPR will be not any longer critical but rather it will be the new desired frequency nadir time.

$$P_{IBFPR}(t) = \frac{\Delta P * (1 - t_{cr}/t_{nadir}) * t}{t_{cr}} \tag{6}$$

According to the obtained expression in Equation (6); it can be realized that the desired power response from the inverters depends exclusively on parameters that cannot be directly measured from the grid connecting point. In a real situation the values of ΔP, t_{nadir} and t_{cr} cannot be known in advance, representing these factors a challenge in the implementation of this ideal power response. Those values are dependent on the grid characteristics, the primary conventional reserve deployment time and the overall system inertia [16]. Thus, two main cases are considered for the remaining analysis with the intent of covering a wider range of systems with different characteristics and dimensions.

2.3. Simulation Cases

As presented in the previous section, the values of critical time and frequency nadir depend on the system imbalance and primary reserve deployment time. In spite of assessing the influence of the grid size and the primary reserve characteristics, two main cases are considered. In both cases is assumed that the initial steady frequency is the nominal 50 Hz.

- **Small scale grid case:** For the evaluation a well-known and studied benchmark grid topology as the WSCC model, also known as the IEEE 9 bus model, is considered. Synchronous reserve deployment is in the order of a few seconds due to governor response [9,17]. To assess the typical simplifications made in power system analysis, two approaches of these cases were developed:

  Scenario A - Simplified Model: The power system is represented by an equivalent single machine model in which losses are neglected. In this case, typical governor data is considered. It is investigated the critical time for inverters activation and the required IBFPR is also determined. Furthermore, the impact of synthetic inertia is analyzed.

Scenario B - Extended Model: All the power system components (transmission lines, transformers, exciters and governors of the three generators) and its dynamic characteristics are considered in the IEEE 9 bus model for critical time and IBFPR estimation.

- **Large scale grid case:** The European grid-scale in which all the synchronous machines are modeled and simplified as one single machine, provided with the characteristic expected from the overall system. Synchronous primary reserve deployment is in the order of $\sim$ 30 s [4,18]. The frequency response is assumed to be the same that the European response analyzed by ENTSOE [4]. Similarly, as in the simplified model of the IEEE benchmark, the influence of synthetic inertia and IBFPR is evaluated.

Table 2. : Summary of the simulated cases

Cases	**Assessment**	
	IBFPR	Synthetic Inertia
Small scale grid		
a) Simplified IEEE model	X	X
b) Extended IEEE model	X	
Large scale grid	X	X

Therefore with the selected cases, the critical and nadir time are estimated through the simulation of different scenarios combining a range of imbalances and shares of non-synchronous generation. In order to assess Equation (6), a fit of the critical time as function of RoCoF is carried out. With the corresponding fit function for each case, Equation (6) can be easily applied assuming that the inertia of the system is known and power imbalance can be calculated as: $\frac{df}{dt}\frac{T_a P_{LOAD}}{f_0}$.

2.4. Simplified IEEE 9 bus Model

As a first step to evaluate the impact of inverter-based generation and power imbalances in the grid, the whole system is simplified as one single generating unit; neglecting all losses in the system (Transformers, transmission lines and generators) with the assumption that the mechanical output of the prime mover is the same than the electrical power output at generator terminals. Table 3 provides a summary of the elements comprising the base model.

Table 3. : Elements of the IEEE 9 bus model.

	Quantity
Buses	9
Transformers	3
Transmission Lines	6
Generators	3
Load	315 MW

Figure 3 is the block representation of the swing equation (1), it only differs in the fact that blocks representing the inverter-based generation have been included. The mechanical power is represented by the output of a steam turbine governor model, which is used to represent the synchronous machine as depicted in Figure 4. When equilibrium is lost, the accelerating power is multiplied by the transfer function $1/(2HS)$, where H is the machine inertia constant and S is the machine power rating. From Equation (1) this product equals the derivative of frequency, therefore an integrator block is added to obtain the frequency response [9,19,20]. A feedback loop is added and an error signal obtained from the reference frequency so the synchronous machine can react as frequency deviates from nominal.

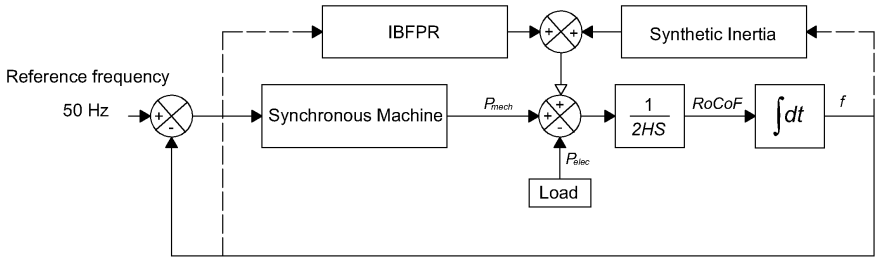

Figure 3. Simplified representation of the IEEE 9 bus model. Blocks linked by the solid line represent the conventional swing equation given by Equation (1). Represented with dashed lines the respective frequency signals to the blocks of IBFPR and synthetic inertia, which add power to the system.

The values of kinetic energy and time constants of a synchronous machine of 835 MVA were selected to represent the synchronous response, with the load of 315 MW the system acceleration time constant is 14 s, which is approximately today's Europe acceleration constant [4]. This is the base scenario where a 100% synchronous generation is assumed. For the sake of evaluating the impact of the penetration of inverter-based generation; the values of lower capacity generators were selected, diminishing the total system inertia.

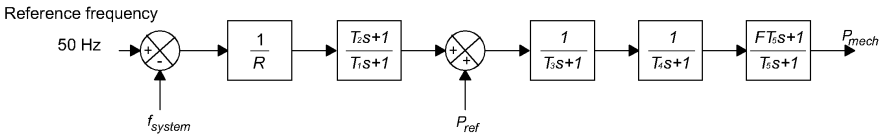

Figure 4. Model of the general-purpose governor for the representation of synchronous machines; where R is the turbine droop, P_{ref} is the reference load at nominal frequency, T_1 is the governor delay, T_2 is the reset time constant, T_3 is the servo time constant, T_4 is the steam valve time constant and T_5 is the steam re-heat time constant [21].

Table 4. : Typical generator values and governor settings as function of capacity [21]

Parameters	**Generator Capacity (MVA)**										
	911	835	590	410	384	192	100	75	51.2	35.29	25
T_1 (s)	0.1	0.18	0.08	0.18	0.22	0.083	0.09	0.09	0.2	0.2	0.2
T_2 (s)	0	0.03	0	0	0	0	0	0	0	0	0
T_3 (s)	0.2	0.2	0.15	0.04	0.2	0.2	0.2	0.2	0.3	0.3	0.3
T_4 (s)	0.1	0	0.05	0.25	0.25	0.05	0.3	0.3	0.09	0.2	0.09
T_5 (s)	8.72	8	10	8	8	8	0	0	0	0	0
Kinetic Energy (MWs)	2265	2206.4	1368	1518.7	1006.5	634	498.5	464	260	154.9	125.4
H (s)	2.486	2.642	2.319	3.704	2.621	3.302	4.985	6.187	5.078	4.389	5.016
P_{max} (MW)	820	766.29	553	367	360	175	105	75	53	36.1	22.5
T_a (s)	14.381	14.009	8.686	9.643	6.390	4.025	3.165	2.946	1.651	0.983	0.796

Even though load imbalances up to 40% were simulated in each inertia scenario, for estimation of the critical time the power capacity limit of the generators was disregarded. The negative imbalance was simulated by increasing the system load.

2.5. Extended IEEE 9 bus Model

Since it is desired to compare the results obtained in Section 2.4 against some model that takes into account the whole system components, losses, and dynamics; an extended representation of the IEEE 9 bus model was implemented in Simulink [22]. In this representation, simulations for different values of system inertia and load imbalance were performed, similarly as it was done with the simplified

representation of the model. Figure 5 shows the extended IEEE 9 bus grid architecture with IBG added.

To evaluate the validity of the equation describing the IBFPR needed to avoid ULFS, the IEEE

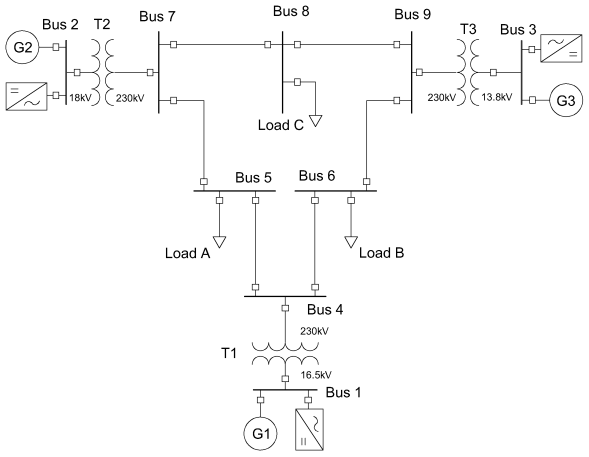

Figure 5. One line diagram of the IEEE 9 bus model. The inverter-based frequency response has been added at the same bus of the generating units.

model was modified with the insertion of ideal controlled power sources blocks, which were set up to inject power into the grid accordingly to the simulated scenario. Therefore, no means of frequency measurement were included and only IBFPR was assessed. As it was done in Section 2.4, the total acceleration time constant of the system equals 14 s when there is no share of non-synchronous generation. Hence the same kinetic energy should be distributed among the three generators' rotating masses in the extended model as in the simplified representation. From Equation (7) it can be easily calculated that the system kinetic energy with 14 s of acceleration time constant is 2205 MWs.

$$T_{sys} = 2 * E_k / P_{load} \tag{7}$$

Since the inverter-based generation reduces the system kinetic energy; for different levels of inverter-based generation, the generator nominal capacity was kept constant and the inertia constant of each machine multiplied by the synchronous share factor fss. The total kinetic energy of the system is the summation of all units.

To start the simulations in steady-state conditions, a load flow calculation of the grid was carried out to calculate the initial conditions for the exciter and prime mover models. Table 5 summarizes the main values for setting the system initial conditions; acquired from the power flow tool provided by SIMSCAPE.

Table 5. : Steady state initial conditions of the system

Bus number	Bus Type	Voltage (pu)	Active Power (MW)	Reactive Power (MVAr)
1	Slack	$1.04 \angle 0°$	72.2	25.64
2	PV	$1.025 \angle 9.83°$	163	8
3	PV	$1.025 \angle 4.63°$	85	-9.41
5	PQ	$0.9949 \angle -4.42°$	125	50
6	PQ	$1.01211 \angle -4.16°$	90	30
8	PQ	$1.0172 \angle 0.17°$	100	35

2.5.1. IBFPR Representation

The IBFPR was modeled as controlled current sources. These controlled sources inject active power according to the load imbalance and system inertia simulated. The continuous measurement of voltage is required to determine the amount of current needed to supply the requested power. The

IBFPR will have symmetrical and balanced characteristics. Due to this reason, the magnitude and angle of the current phasor will be obtained from the positive sequence of the measured voltage. From the definition of complex power and voltage symmetrical components in three-phase systems (8), the positive sequence components of phase voltage and line current are obtained [19].

$$S^1_{3\varphi} = 3 * V^1_{LN} * \bar{I}^1_L \tag{8}$$

This equation is valid for RMS values of voltage and current in which $S^1_{3\varphi}$ is the positive sequence of the three-phase complex power, V^1_{LN} is the positive sequence of voltage line to neutral and $\bar{I}^1_L$ is the conjugated of the positive sequence line current. Nevertheless, the measured voltage values in Simulink are peak voltages, then the equation for power and current become:

$$S^1_{3\varphi} = \frac{3 * V^1_{LNpeak} * \bar{I}^1_{Lpeak}}{2} \tag{9}$$

$$I^1_{Lpeak} = \frac{2 * \bar{S}^1_{3\varphi}}{3 * V^1_{LNpeak}} \tag{10}$$

With the help of the **a** operator ($-0.5 + j\sqrt{3}$ or $1\angle 120°$) the values of the positive sequence component of phase voltage can be obtained.
From $V_a + V_b + V_c = 0$ and $V^1_a = \frac{V_a + aV_b + a^2V_c}{3}$:

$$\begin{aligned} V^1_a &= \frac{V_a + aV_b - a^2V_b - a^2V_a}{3} \\ &= \frac{V_a * (1 - a^2) + aV_b * (1 - a)}{3} \end{aligned}$$

Since $V^1_{an} = \frac{V^1_a}{\sqrt{3}\angle 30°}$, $\sqrt{3}\angle 30° = 1 - a^2$ and $\sqrt{3}\angle -30° = 1 - a$ then after some algebraic manipulation the expression for V^1_{an} becomes:

$$V^1_{an} = \frac{V_a - a^2V_b}{3} \tag{11}$$

With the obtained expressions for the positive sequence of phase voltage (11) and complex power (9), the needed current (10) to supply the IBFPR related to the measured voltages can be implemented in Simulink as depicted in Figure 6. The ramping function will last until the critical time is reached, afterward, the IBFPR output will remain constant.

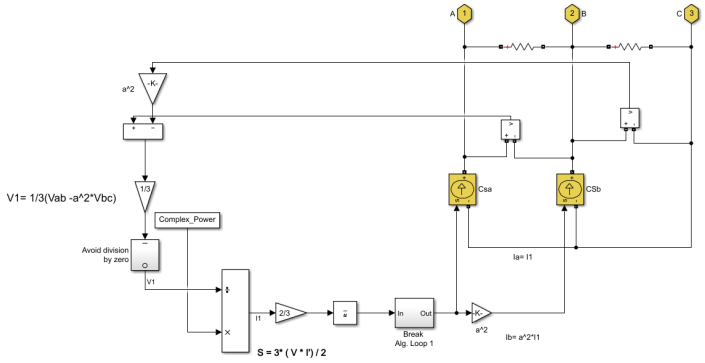

Figure 6. Implementation of IBFPR in the extended IEEE model. From the voltages readings of lines a-b and b-c the voltage V_{an} is calculated using Equation (11), then Equation (10) is implemented to calculate the current to be fed into the system using the complex power response obtained using Equation (6) and the previous calculated value of V_{an}.

It must be noticed that when the IBFPR depicted in Figure 6 was implemented in Simulink, additional blocks were added to run the simulation, such blocks are a break algebraic loop just before the conjugate block. Additionally, a block to avoid division by zero was added at the output of the gain of 1/3.

2.6. Large Scale Case: Europe Power System

Under normal operation, ENTSOE has reported values of RoCoF in the range of 5-10 mHz/s for power outages of 1 GW in the current interconnected power system. If an imbalance event of more than 3 GW occurs with depleted primary reserve, extraordinary values of frequency and RoCoF might be reached. After serious disturbances, the Continental European Power System has experienced RoCoF between 100 mHz/s and 1 Hz/s. Imbalances of 20% or more along with RoCoF greater than 1 Hz/s have been determined by experience to be critical [4]. ENTSOE has determined that the reference scenario (loss of 3 GW generation with 150 GW load and 2%/Hz self-regulation) in the interconnected operation, the influence of inverter-based generation, and therefore, the reduction of system inertia would not jeopardize system stability. Due to the expected increase of non-synchronous generation in the future, international power trade and renewables variability; ENTSOE estates in its future split reference scenario that the power system must be capable of withstanding imbalances greater than 40% with RoCoF of 2 Hz/s or higher. Under these circumstances, the resulting islands must avoid load shedding. Hence, the conditions of the split scenario are considered for further analysis.

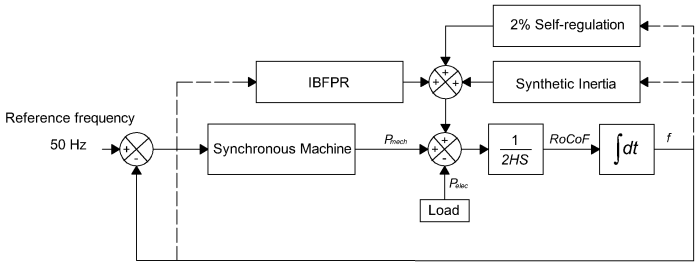

Figure 7. Large scale grid derived from the simplified IEEE model. The synchronous response was modified to match the European reserve response and the effect of self-regulation was added.

To fit the behavior of the system to the one modeled by ENTSOE, the synchronous representation in the simplified IEEE model shown in Figure 4 was used as a base to emulate such behavior; this was done with the insertion of an additional block at the output of the governor model. With this approach, the primary power reserve can be easily tuned with the assistance of the Control System Tuner App available in MATLAB. The time of utmost interest for analysis is from the inception of the power imbalance until the nadir time. Therefore, the system must perform as similar as possible in this region compared to the ENTSOE reference, whereas after the nadir time, the disparity between responses can be neglected. On the European scale, the reserves must be completely deployed within 30 s after the occurrence of the disturbance.

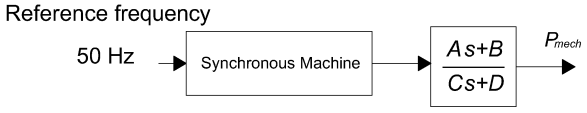

Figure 8. Governor representation for the large grid scale case. The synchronous machine block represents the governor model used in Section 2.4. The Control System Tuner App sets the constants A, B, C and D of the additional block in the model in order to have a step response with a rise time of $\sim 30s$ by establishing an overshoot of 2% and a time constant of 8 seconds [20].

2.6.1. System Parameters

When a power system of n number of synchronous machines is assumed; having each of them a capacity S in MVA, a nominal power P_{nom} in MW and supposing that each machine operates at a de-load factor dl of P_{nom}; with an acceleration constant equal to T_{nom} then the number of machines n, for the load $P_{syncload}$ served by synchronous machines is:

$$n = \frac{P_{syncload}}{P_{nom} * dl} \tag{12}$$

The time acceleration constant of the system T_{sys} can be obtained as follows:

$$\begin{aligned} T_{sys} &= \frac{\sum_{i=1}^{n} P_i * T_i}{P_{LOAD}} \\ &= \frac{nP_{nom} * T_i}{P_{LOAD}} \\ &= \frac{P_{syncload} * T_{nom}}{P_{LOAD} * dl} \\ &= \frac{Syncshare * T_{nom}}{dl} \end{aligned} \tag{13}$$

In this sense the system acceleration time constant can be calculated with a synchronous share of 100%, resulting in $T_{sys} = 12.5s$ with values of $T_{nom} = 10s$ [4,21], and a de-load factor $dl = 0.8$. Considering only the swing equation, it can be demonstrated that RoCoF and therefore the frequency response of the system is only dependent on the percentage of load imbalance and the system acceleration time constant. From the definition of RoCoF as $\frac{df}{dt} = \frac{\Delta P * f_0}{2 * E_k}$ and $T_{sys} = \frac{2 * E_k}{P_{LOAD}}$:

$$\begin{aligned} \frac{df}{dt} &= \frac{\Delta P * f_0}{P_{LOAD} * T_{sys}} \\ &= \frac{\Delta P_{pu} * f_0}{P_{LOAD} * T_{sys}} \end{aligned} \tag{14}$$

In Equation (14) the value of ΔP_{pu} is the normalized value of power imbalance having as base power the value of load P_{LOAD}.

3. Results

3.1. Analysis of Critical Time

When the simplified and the extended models of the IEEE benchmark are compared for the estimation of the critical time in Figure 9, it is noticed a higher deviation in the low range of RoCoF. This because in this range of RoCoF the critical time is long enough to allow the governor response activation of the respective synchronous machines representation. Therefore it can be stated that the simplifications made in the model have a greater influence on the results for low values of penetration of IBG and low power imbalances; in this sense, the simplifications become less significant as the RoCoF increases in such a manner that the activated synchronous reserve is not relevant in frequency support. In the range of RoCoF higher than 2 Hz/s the critical time trend for the European grid-scale and the simplified IEEE model get closer each to other as RoCoF increases.

Therefore under high RoCoF conditions in any of the models, the primary reserve does not significantly counteract the frequency drop [3]. Figure 9 demonstrates that primary reserve can be neglected for determining the critical time when the combination of IBG and load imbalances would lead to high values of RoCoF; as it increases, the approximation of critical time as 1 Hz/RoCoF narrows the difference with the results obtained from simulations [8]. Nevertheless, such simplification applies

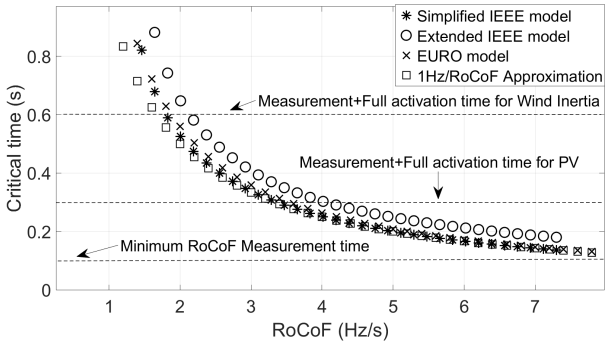

Figure 9. Results for critical time in all simulated models with a penetration of IBG of 80% .

to the simplified IEEE model and the European-scale grid model. Hence, the influence of all the dynamics and machine components, such as the generator exciter and damping windings, seems to improve the critical time. The damping torque was not considered in Equation (1) for the simplified IEEE model; the inclusion of such may lead to more accurate results when compared with the extended model.

Table 6. : Critical time for European-scale case given in seconds.

IBG share (%)	**Load Imbalance (%)**							
	3	4	5	6	7	8	9	10
20	-	-	6.081	4.517	3.629	3.050	2.638	2.316
40	-	6.226	4.169	3.215	2.628	2.222	1.934	1.705
60	7.142	3.639	2.623	2.062	1.698	1.451	1.263	1.122
80	2.753	1.744	1.277	1.018	0.843	0.722	0.628	0.559
95	0.697	0.436	0.322	0.254	0.211	0.179	0.157	0.140

Because the characteristics of the European interconnected scenario provided by ENTSOE were assumed to be the same as the resulting islands after a severe event; the results for the large scale model can be understood as the behavior of the whole European system with bigger perturbations. The reference scenario assumes a power imbalance of 3 GW, which corresponds to a 2% of the 150 GW load [4]. If in the future a bigger reference scenario is utilized, then the synchronous response would not be enough to balance the system before load shedding occurs. Table 6 exhibits the required time when the power imbalance is increased by up to 10% for different IBG penetration.

3.2. Analysis of Synthetic Inertia and Fast Power Reserve

3.2.1. Effect Synthetic Inertia on Frequency

In this section, the results of the implementation of synthetic inertia in the simplified IEEE model and the European model are presented. The frequency nadir for such systems without any additional power support apart from synchronous response are illustrated in Figures 10a and 10b.

In any of the cases, UFLS is not avoided for all combination of imbalances and acceleration constants with the application of synthetic inertia. It can also be observed in Figure 11a that values of frequency nadir under 49 Hz are reached for imbalances bigger than 14% combined with shares of IBG above 80% in the simplified representation of the IEEE model. Nevertheless, enhanced performance is observed in the simplified IEEE model. The reason behind this is the faster response of the synchronous share present in the system, which jointly performs with the synthetic inertia to improve overall frequency response performance. On the other hand, the frequency nadir of the European scale model, depicted in Figure 11b at 80% of IBG, reaches 48.89 Hz with an imbalance of 3%. This demonstrates

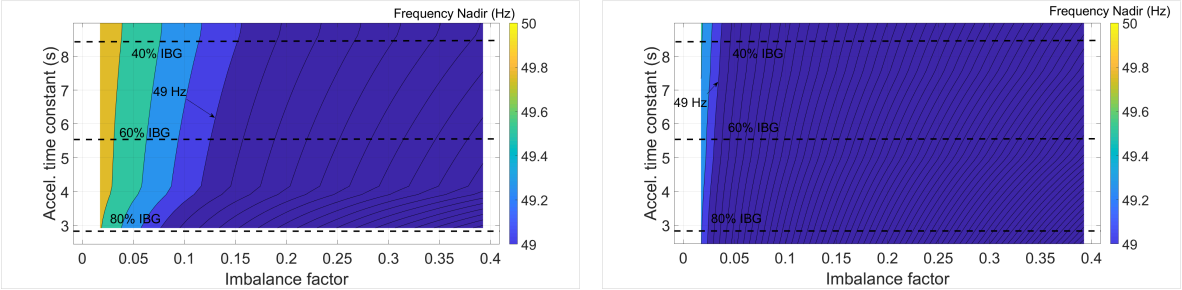

(a) Simplified IEEE model **(b)** European-scale model

Figure 10. Frequency nadir with no support from IBG. (**a**) The frequency nadir of the simplified IEEE model. For the time acceleration constant corresponding to the 80% of the IBG, the frequency nadir reaches values lower than 49 Hz with power imbalances starting at $\sim$ 7%. In (**b**) the frequency nadir of the European-scale grid is illustrated. At 80% of IBG the frequency nadir reaches 48.73 Hz with only $\sim$ 3% of imbalance.

that synthetic inertia is not enough by itself for withstanding severe imbalances under high penetration of inverter-based generation.

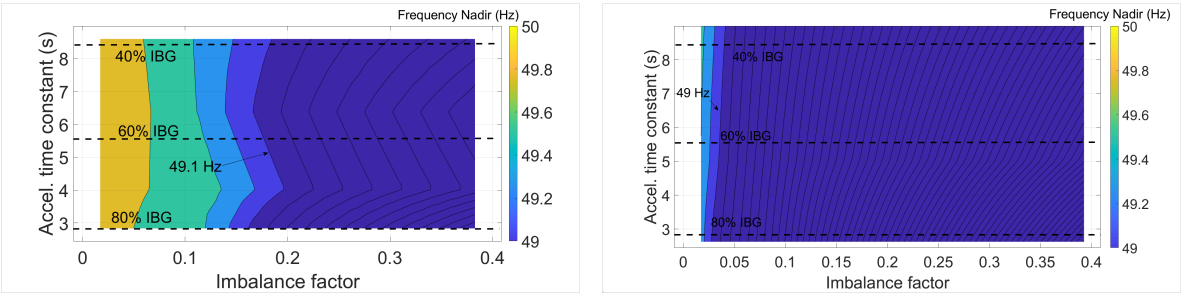

(a) Simplified IEEE model. **(b)** European-scale model.

Figure 11. (**a**) Shows the frequency nadir once synthetic inertia has been applied to the 40% of the IBG in the simplified IEEE model. (**b**) Frequency nadir of the large scale model with the same share of contribution from synthetic inertia.

Figure 12a and 12b indicate the frequency response obtained of the system with an non-synchronous generation of 80% for different load imbalances. In Figure 12a can be observed how the frequency drops below 49 Hz with a 10% of imbalance when no IBFPR or synthetic inertia is used as a frequency support strategy. In the same figure, the frequency responses for different levels of synthetic inertia is presented. It is noticed the improvement in the response with the implementation of synthetic inertia. UFLS is avoided for every share of synthetic inertia, assuming that primary reserve takes place after synthetic inertia. As the imbalance increases, the effectiveness of the synthetic inertia decreases.

Figure 12b shows how a contribution of wind power of 40% from the inverter-based generation is capable of avoiding UFLS. Nevertheless with the share of 80% the frequency drops smoothly during a short period, then suddenly the frequency drops below 49 Hz. This situation leads to UFLS after 10 s because frequency has been sustained during that time by the synthetic inertia power. Since 10 seconds is the assumed time limit for exceeding the nominal turbine power rate; the synthetic inertia power, which has a big contribution to counteract the power imbalance, is switched off. On the other hand, when a higher imbalance occurs and the synthetic inertia response is saturated, due to the limitation of 10% of rated power, the mechanical power increases at 10 seconds, having a less severe impact the switching off of the inertial response.

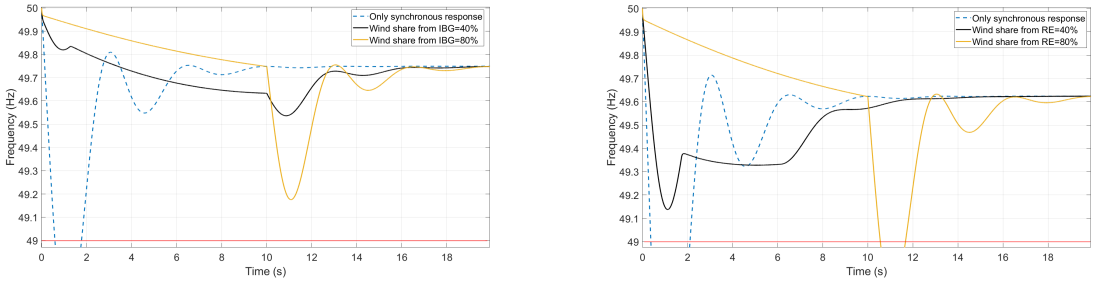

(a) Simplified IEEE model with 10% imbalance **(b)** Simplified IEEE model with 15% imbalance

Figure 12. Cases with contribution of 40% and 80% of the total IBG share are compared with the scenario with no support coming from IBG.

3.2.2. Effect of Power Ramp Response on Frequency

The contribution from the ramping power in diminishing system RoCoF from the inception of the perturbation until the critical time was disregarded when Equation (5) was calculated. Assuming an instant switch-on of the IBFPR at the critical time, the frequency nadir would be 49 Hz. How ever, a ramp power response was assumed instead. Therefore the frequency response of an unbalanced system commonly exhibits a frequency nadir higher than 49 Hz due to the contribution of the ramping period. In this sense, it can be inferred that the longer the ramping period, the higher the frequency nadir that will be obtained. On the other hand, with the faster activation of IBFPR, the ramp slope and the steady power output can be diminished compromising frequency nadir.

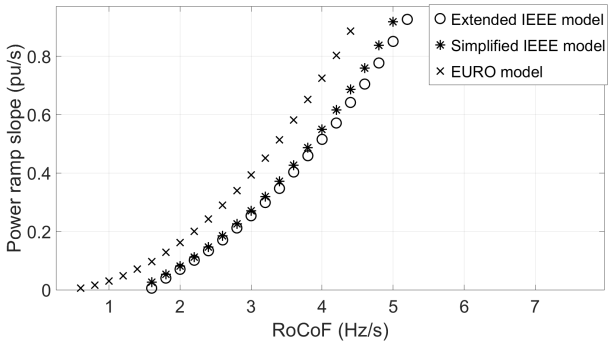

Figure 13. Comparison of the results of the three models in terms of the IBFPR power ramp which is needed at 80% of share from non-synchronous generation.

When a comparison is established between all the calculated power ramp slopes in per unit (pu), it can be noticed that with a high penetration of non-synchronous power in the system, the required power to ensure no UFLS have a consistent trend between the three models and proximity as seen in Figure 13. A bigger amount of power ramp slope is needed in all the range of RoCoF for the European case. After inspecting Equation 6 it is noticed that the IBFPR is affected by the factor $1 - t_{cr}/t_{nadir}$, then as nadir time increases, IBFPR increases as well. The nadir time for the European case, due to the action of the self-regulation and primary reserve deployment of 30 seconds, is in the range of 3-12 seconds (6 seconds for 80% IBG penetration) whereas the nadir time for the simplified IEEE model is between 1-3 seconds.

3.2.3. Fast Power Reserve

The required power ramp to avoid load shedding has been found for both IEEE 9 bus models and the European-scale model. Hence, the IBFPR at the critical time, which remains constant after the critical time, would be accounted as the fast power reserve. In Table 7 the required values for the inverter base reserve for the European model are listed for imbalances out of the reference case of

ENTSOE.

Table 7. : Fast power reserve in per unit for the European case. Power reserve expressed in pu with power load as the base

IBG share (%)	Load Imbalance (%)							
	3	4	5	6	7	8	9	10
20	-	-	0.025	0.038	0.049	0.060	0.070	0.081
40	-	0.016	0.030	0.041	0.052	0.063	0.073	0.083
60	0.005	0.024	0.035	0.045	0.056	0.066	0.077	0.087
80	0.016	0.028	0.039	0.049	0.062	0.070	0.080	0.09
95	0.024	0.035	0.045	0.055	0.065	0.075	0.085	0.096

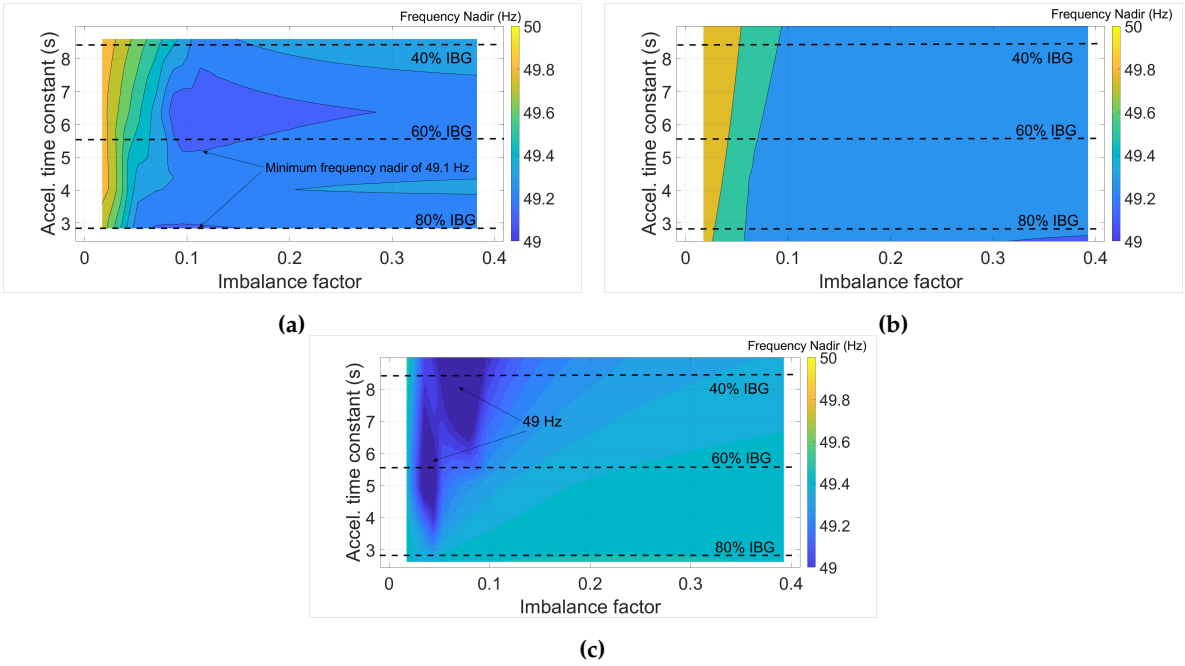

Figure 14. Frequency nadir with the implementation of IBFPR in: (**a**) The simplified IEEE model (**b**) The extended IEEE model. (**c**) The large scale (European model).

When IBFPR is implemented in all three cases, frequency drop below 49 Hz is avoided for almost all values of RoCoF, provided that enough IBFPR is available for the given imbalance. Figures 14a to 14c show the frequency nadir for all the cases.

It can be observed that in the IEEE grid models, depicted in Figure 14a and 14b, that UFLS is avoided in all the cases. However, in the simplified IEEE model, a minima area with a value of 49.1 Hz is found as indicated in the figure. This is caused due to the selected values of time constants for such inertia scenario. As indicated in Table 4 the generator with a capacity of 590 MVA has a bigger reheat time constant than the other machines, causing a delay in synchronous response. As the imbalance increases, the relevance of such response diminishes, therefore frequency nadir increases. In the case of the extended IEEE model, time constants were kept equal for all inertia scenarios and only generator inertia was changed. In the European-scale model depicted in Figure 14c, UFLS is not avoided in the region of low imbalance and high acceleration time constant. Since the implemented IBFPR was based on a power response as a function of the measured RoCoF, the inaccuracy in the fit function leads to overestimating the critical time in the low region of RoCoF. This has a bigger influence on the

366 European-scale model because such inaccuracy is not compensated by a faster power response from
367 the synchronous machines.

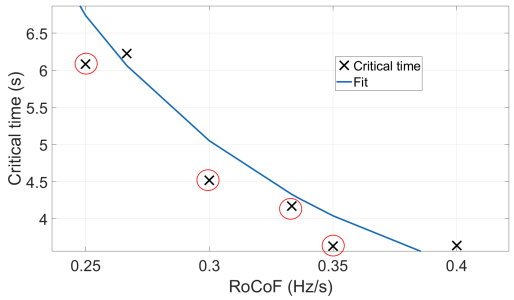

Figure 15. Overestimation of critical time leading to UFLS in the European-scale model.

368 *3.3. Synchronizing effect, lack of damping torque and implications*

369 The diminishing of synchronous machines in the system leads to a very weak network where
370 synchronizing and damping torque, which are inherent characteristics of synchronous machines,
371 are not enough to stabilize the system [9]. Although the implementation of IBFPR contributes to
372 keeping the synchronous machine on step, oscillations in the speed/frequency response of the rotor
373 are observed. These oscillations are created by the lack of damping torque which is provided mainly by
374 the synchronous machines through damping windings, rotor field exciter, and power system stabilizer
375 [9].

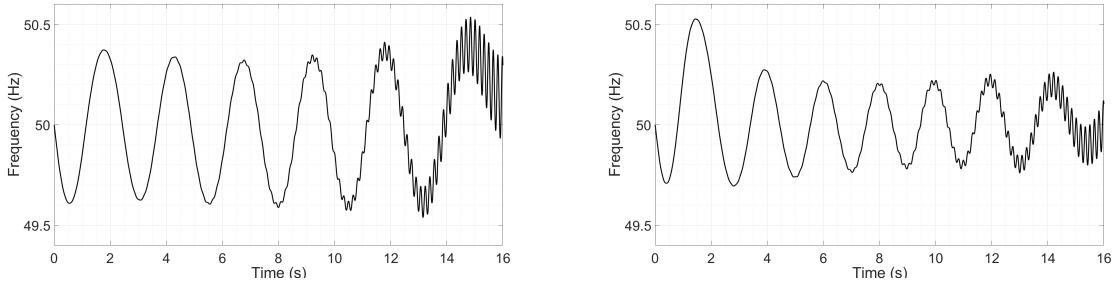

(a) Without IBFPR **(b)** With IBFPR

Figure 16. In (**a**) the oscillatory frequency response is depicted when no additional frequency support is given by the IBG, whereas in (**b**) the IBFPR is applied. In both cases an imbalance of 2% and a penetration of 95% of IBG were considered.

376 For the simplified IEEE model and the European-scale model, only transfer functions describing
377 an equivalent system governor were considered. Hence in such approaches, the effect and dynamics
378 of synchronous generator's exciters and inter-machine interaction were not taken into account. The
379 before mention factors influence greatly small signal stability [9,21]. Even though the scope of this
380 work was to analyze the power-time characteristics needed to avoid frequency collapse; oscillations
381 were observed but they could not be addressed by the simple injection of power to the system. When
382 penetration of 95% of inverter-based generation and 2% of load imbalance is considered, UFLS is not
383 reached but the system becomes unstable as shown in Figure 16a and Figure 16b. With penetrations
384 levels above 85%, complete frequency stability is not ensured with the injection of fast power reserve.
385 Then the system becomes unstable with increasing amplitude oscillations. It is important to note
386 that ENTSOE in its EUROPEAN interconnected scenario determined that there is no UFLS when an
387 imbalance of 2% with a high contribution of non-synchronous generation occurs. Nonetheless, no
388 inter-machine interaction was considered and therefore a similar effect as the one in 16a could be
389 experienced.

4. Discussion

Conventional synchronous machines were found not to be able to ensure transient frequency stability in conditions of power imbalance exceeding 2% in the case of the European model. The governor's operation is by far too slow to constitute the unique solution for frequency support during the transient period. Inverter based fast power reserve would be needed to be activated in an extremely short time. Some extended capability to withstand power imbalances is observed with the faster governor response in the IEEE models.

Although unlikely to occur, the consideration of the uncertainty of synchronous reserves availability and possible power transmission congestion in future scenarios could lead to higher imbalances as nowadays [3]. To avoid load shedding in penetration scenarios above 80% of non-synchronous generation for and load imbalances up to 40%, inverter-based fast power reserve must be deployed over time in the order of 100-500 ms, independently of grid size and primary reserve response. Nevertheless, today's full power activation time of renewable sources without storage is in the range of 200 to 600 ms. Table 8 lists some important and typical time scales of the most common power electronic technologies implemented in modern power systems[1]. These activation times are adequate for power imbalances leading to values of RoCoF equal or less than 4 Hz/s as studied by ENTSOE in future scenarios [4]. Hence with today's frequency measuring time and power deployment from renewable sources; load shedding and possible total blackouts would not be avoided in scenarios with plenty of renewables and high expected imbalances. Storage would be a key factor to avoid de-loading and curtailment of renewables, the fast activation times (<50 ms) and promising price reduction make storage a good strategy to provide power balancing in both over and under frequency cases [23]. A comprehensive method for the estimation of the required time for the activation of the inverter-based reserve was developed in this paper, with such method a frequency support strategy for inverters can be implemented for an expected level of imbalance as long as system inertia is monitored or estimated.

Table 8. : Activation times for fast power reserve of non-synchronous technologies [8]

Technology	Full Fast Frequency response (ms)
Wind turbine-Synthetic inertia	$\sim$ 500
Lithium batteries	10-20
Flow batteries	10-20
Lead-acid batteries	40
Flywheels	<4
Super capacitor	10-20
Solar PV	100-200
HVDC	50-500

Synthetic inertia from wind turbines has a better performance when operated along with fast synchronous response systems as shown in section 3.2.1 with the simplified IEEE model. When synthetic inertia is implemented with slower response primary response such as the case of the large scale of the European grid, it was not noted an appreciable improvement in regards to the frequency nadir. Therefore, synthetic inertia is not able by itself to regulate or restore frequency deviation [15]. This predictable outcome limits its usage just for slowing down the frequency drop after a load event. The influence of the gain K_i is fundamental since the choice of a specific value can avoid load shedding just for a certain range of imbalances. For instance, in Section 3.2.1 it was demonstrated that the

[1] Times required for the all measurement, signal transmission and processing and coordination of power electronic device's controls [8].

chosen value for K_i is adequate for imbalances of 10% but as the imbalance increases to 15%, the initial dependency of system to sustain the imbalance from the synthetic inertia makes the frequency to rapidly drop after 10 seconds, when the synthetic inertia has been removed. A proper selection of K_i can stabilize the system or the progressive reduction of synthetic inertia power could extend synthetic inertia effectiveness.

If the reference scenario for the primary reserve is increased in the European context, the synchronous response is not fast enough for imbalances higher than 2%. Full activation time in the range of 0.14 and 2.75 seconds would be required for the fast power reserve for penetrations of non-synchronous generation above 80% and imbalances between 3 and 10%. Additionally, the fast power reserve would be almost equivalent to the imbalance, meaning that almost no contribution from synchronous machines is obtained. Although UFLS is avoided in the extended model in scenarios with penetrations of non-synchronous generation above 85% with injection of inverter-based fast power reserve; total system stability is not ensured after a few seconds ($\sim 5s$), due to the presence of un-damped oscillations provoked by the poor damping torque present in the system as consequence of synchronous share reduction. Even though the approach considered throughout this work was the fast power reserve deployment to avoid under-frequency load shedding. If the same frequency deviation from nominal is considered as critical for the over-frequency case (51 Hz); the same values would be obtained for critical time and power response. The difference lies in the power flow direction, in this case, power surplus should be removed from the grid or converter to another form of energy, like electrochemical storage. When a linear system is employed as the cases of the simplified IEEE model and the large scale scenario, no difference was found between the critical time for under and over-frequency. When the non-linearity of the system is included in the extended model, the critical times between under and over-frequency do not match as illustrated in Figure 17

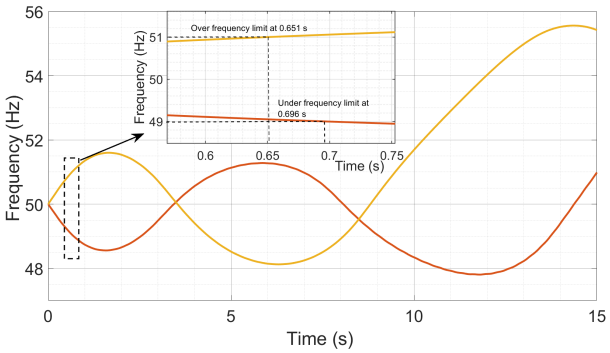

Figure 17. Under and over-frequency events in the extended IEEE model, a difference of 45 ms between each critical time is found.

In general, similar behavior is exhibit from the different models and approaches, even though they differ considerably in size and complexity. Hence, the simplified block representation of the power system seems to be a fair way to sketch overall system trends and responses. The differences among governors' time constants were found to be not significantly influential in frequency studies. The difference in critical time estimation between a full grid simulation and a simplified model was calculated to differ between 20-35%, such difference could be crucial in fast power reserve studies and therefore should be considered when precise applications are implemented. A comprehensive method for estimation of the inverter-based fast power reserve and critical time were developed and proved through the implementation in the two cases.

Author Contributions: For research articles with several authors, a short paragraph specifying their individual contributions must be provided. The following statements should be used "conceptualization, X.X. and Y.Y.; methodology, X.X.; software, X.X.; validation, X.X., Y.Y. and Z.Z.; formal analysis, X.X.; investigation, X.X.;

resources, X.X.; data curation, X.X.; writing–original draft preparation, X.X.; writing–review and editing, X.X.; visualization, X.X.; supervision, X.X.; project administration, X.X.; funding acquisition, Y.Y.", please turn to the CRediT taxonomy for the term explanation. Authorship must be limited to those who have contributed substantially to the work reported.

Funding: Please add: "This research received no external funding" or "This research was funded by NAME OF FUNDER grant number XXX." and and "The APC was funded by XXX". Check carefully that the details given are accurate and use the standard spelling of funding agency names at https://search.crossref.org/funding, any errors may affect your future funding.

This research received no external funding

Conflicts of Interest: The authors declare no conflict of interest.

Abbreviations

The following abbreviations are used in this manuscript:

ENTSOE	European Network of Transmission System Operators for Electricity
FPR	Fast Power Reserve
HVDC	High Voltage Direct Current
IEEE	Institute of Electric and Electronic Engineers
IBFPR	Inverter based Fast Power Reserve
IBG	Inverter Based Generation
PV	Photovoltaic
RoCoF	Rate of Change of Frequency
SI	Synthetic Inertia
UFLS	Under Frequency Load Shedding
WSCC	Western System Coordinated Council

References

1. Agora Energiewende. Energiewende: What do the new laws mean? Ten questions and answers about EEG 2017, the Electricity Market Act, and the Digitisation Act.
2. Energiewende, A. Flexibility in thermal power plants–With a focus on existing coal-fired power plants. *Berlin: Agora Energiewende* **2017**.
3. Deutsche Energie-Agentur GmbH (dena) – German Energy. dena Ancillary Services Study 2030: Security and reliability of a power supply with a high percentage of renewable energy.
4. ENTSOE. Frequency Stability Evaluation Criteria for the Synchronous Zone of Continental Europe **2016**.
5. Hoke, A.F. Fast Grid Frequency Support from Distributed Inverter-Based Resources. Technical report, National Renewable Energy Lab.(NREL), Golden, CO (United States), 2018.
6. Andy Hoke, Mohamed Elkhatib, Austin Nelson, Jay Johnson, Jin Tan, Rasel Mahmud, Vahan Gevorgian, Jason Neely, Chris Antonio, Dean Arakawa, and Ken Fong. The Frequency-Watt Function: Simulation and Testing for the Hawaiian Electric Companies. Technical report.
7. Dreidy, M.; Mokhlis, H.; Mekhilef, S. Inertia response and frequency control techniques for renewable energy sources: A review. *Renewable and sustainable energy reviews* **2017**, *69*, 144–155.
8. Miller, N.; Lew, D.; Piwko, R. Technology capabilities for fast frequency response. *GE Energy Consulting, Tech. Rep.* **2017**.
9. Kundur, P.; Balu, N.J.; Lauby, M.G. *Power system stability and control*; Vol. 7, McGraw-hill New York, 1994.
10. Gevorgian, V.; Zhang, Y..N. Wind Generation Participation in Power System Frequency Response. Technical report, National Renewable Energy Lab.(NREL), Golden, CO (United States), 2017.
11. General Electric International. GE Wind Plant Advance Controls.
12. Nesje, B. The need for Inertia in the Nordic Power System. Master's thesis, NTNU, 2015.
13. E. Muljadi, V. Gevorgian, and M. Singh: NREL.; S. Santoso: University of Texas - Austin. Understanding Inertial and Frequency Response of Wind Power Plants: Preprint **2012**.
14. González Rodriguez, A.G.; González Rodriguez, A.; Burgos Payán, M. Estimating wind turbines mechanical constants. *Renewable Energy and Power Quality Journal* **2007**, *1*, 697–704. doi:10.24084/repqj05.361.

15. Wu, L.; Infield, D.G. Towards an Assessment of Power System Frequency Support From Wind Plant—Modeling Aggregate Inertial Response. *IEEE Transactions on Power Systems* **2013**, *28*, 2283–2291. doi:10.1109/TPWRS.2012.2236365.
16. Ørum, E.; Kuivaniemi, M.; Laasonen, M.; Bruseth, A.I.; Jansson, E.A.; Danell, A.; Elkington, K.; Modig, N. Future system inertia. *ENTSOE, Brussels, Tech. Rep* **2015**.
17. Sundaram, D.; Bhuiyan, M. Comparing and Evaluating Frequency Response characteristics of **2008**.
18. Hultholm, C.; Wägar, N. Optimal reserve operation in Turkey–frequency control and non-spinning reserves. Power-Gen Europe, 2015.
19. Grainger, J.J.; Stevenson, W.D. *Power system analysis*; Vol. 67, McGraw-Hill New York, 1994.
20. Ogata, K. *Ingenieria de Control Moderna (Spanish Edition)*; Prentice Hall, 1999.
21. Anderson, P.M.; Fouad, A.A. *Power system control and stability*, 2nd ed. ed.; Wiley: New York and Chichester, 2002.
22. Delavari, A.; Kamwa, I.; Brunelle, P. Simscape power systems benchmarks for education and research in power grid dynamics and control. 2018 IEEE Canadian Conference on Electrical & Computer Engineering (CCECE). IEEE, 2018, pp. 1–5.
23. IRENA, A. Electricity storage and renewables: Costs and markets to 2030, 2017.